Thermal and Chemical Stability of Thiol Bonding on Gold Nanostars

Mykola Borzenkov,*[,†] Giuseppe Chirico,[†] Laura D'Alfonso,[†] Laura Sironi,[†] Maddalena Collini,[†] Elisa Cabrini,[‡] Giacomo Dacarro,[‡] Chiara Milanese,[‡] Piersandro Pallavicini,*[,‡] Angelo Taglietti,[‡] Claire Bernhard,[§] and Franck Denat[§]

[†]Department of Physics "G. Occhialini", University of Milano Bicocca, piazza della Scienza 3, 20126 Milano, Italy
[‡]Department of Chemistry, University of Pavia, viale Taramelli 12, 27100 Pavia, Italy
[§]Institut de Chimie Moleculaire de l'Université de Bourgogne, UMR CNRS 6302, Université de Bourgogne, 21078 Dijon, France

ABSTRACT: The stability of thiol bonding on the surface of star-shaped gold nanoparticles was studied as a function of temperature in water and in a set of biologically relevant conditions. The stability was evaluated by monitoring the release of a model fluorescent dye, Bodipy-thiol (BDP-SH), from gold nanostars (GNSs) cocoated with poly(ethylene glycol) thiol (PEG-SH). The increase in the BDP-SH fluorescence emission, quenched when bound to the GNSs, was exploited to this purpose. A maximum 15% dye release in aqueous solution was found when the bulk temperature of gold nanostars solutions was increased to $T = 42$ °C, the maximum physiological temperature. This fraction reduces 3−5% for temperatures lower than 40 °C. Similar results were found when the temperature increase was obtained by laser excitation of the near-infrared (NIR) localized surface plasmon resonance of the GNSs, which are photothermally responsive. Besides the direct impact of temperature, an increased BDP-SH release was observed upon changing the chemical composition of the solvent from pure water to phosphate-buffered saline and culture media solutions. Moreover, also a significant fraction of PEG-SH was released from the GNS surface due to the increase in temperature. We monitored it with a different approach, that is, by using a coating of α-mercapto-ω-amino PEG labeled with tetramethylrhodamine isothiocyanate on the amino group, that after heating was separated from GNS by ultracentrifugation and the released PEG was determined by spectrofluorimetric techniques on the supernatant solution. These results suggest some specific limitations in the use of the gold−thiolate bond for coating of nanomaterials with organic compounds in biological environments. These limitations come from the duration and the intensity of the thermal treatment and from the medium composition and could also be exploited in biological media to modulate the in vivo release of drugs.

1. INTRODUCTION

Gold nanoparticles (GNPs) are widely used in chemistry, physics, biology,[1] and medicine[2] due to a number of unique properties.[3,4] These include the light scattering and absorption from localized surface plasmon resonances[3,5] (LSPRs), whose wavelength depends mainly on the nanoparticles size, shape, and to a lesser extent the local dielectric constant.[6,7] The latter is tuned in turn by the solvent and by the GNP surface coating. Besides LSPR, coating also affects GNP stability and its interaction with the environment,[8−10] allowing and enriching GNP use in vitro and in vivo for biosensing and therapy.[2,11,12] The direct interaction of the gold surface with thiols (−SH) and disulfides (−S−S−), forming self-assembled monolayers, is the most widely employed method for grafting a coating on GNPs. This may be either a small molecule or a polymer or a combination of both.[4,13] The formed "Au−S" bond is indeed a thiolate−Au^+ coordinative interaction, with a homolytic strength of ∼40 kcal/mol.[14,15] The thermal and environmental stability of such bonds was investigated first on bulk, flat Au surfaces. Ultrahigh vacuum studies showed that thiols desorbed significantly from flat Au at room temperature, in a 7 days time lap.[16] Desorption of linear alkanethiols from flat Au is significant also when surfaces are dipped in hexadecane at 83 °C, with faster desorption for shorter chain thiols, while at room temperature immersion in 1 M NaOH or HCl does not affect monolayers of octadecanethiol over 24 h periods.[17] On the contrary, immersion of gold monolayers of alkanethiols, hydroxyalkanethiols, and tetra(ethylene glycol) alkanethiols in serum-free or 10% FBS (fetal bovine serum) supplemented culture media at 37 °C for short time (30 min) does not evidence desorption.[18] In addition, under similar conditions (tris-buffered saline solution at 37 °C for up to 7 days), hydroxoalkanethiol monolayers are also stable.[19] Stepping to thiol coatings on colloidal solutions of GNPs, literature evidences that competing thiols can displace grafted thiols on coated spherical GNPs even in water and at room temperature,[20,21] although, depending on the nature of the grafted thiols, poor or nihil displacement may even take place.[22]

Received: October 7, 2014
Revised: July 8, 2015
Published: July 8, 2015

Scheme 1. Formula of PEG-SH (MW = 2000), BDP-SH, and HS-PEG-NH-TR[a]

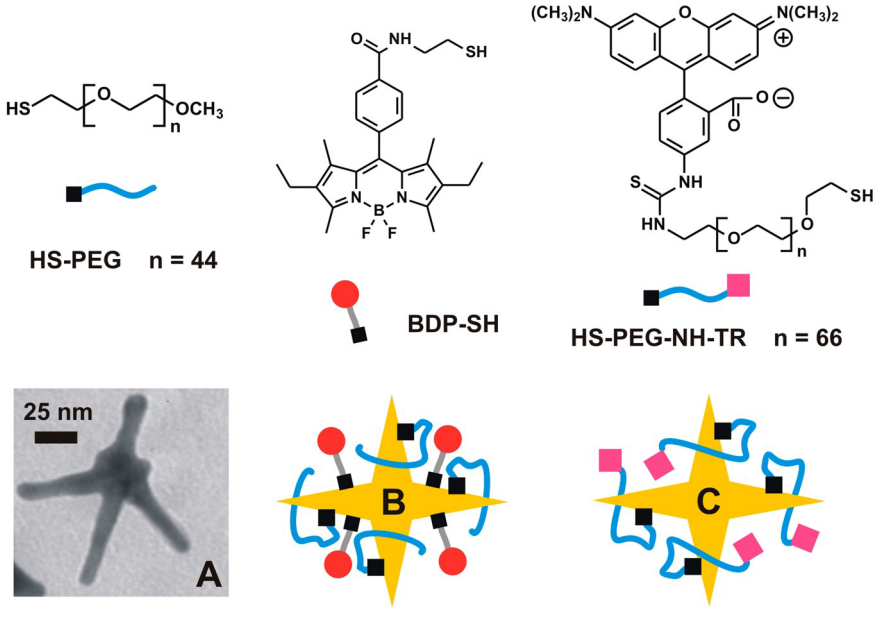

[a] Panel A reports an exemplary TEM image of the used GNSs. Panels B and C are sketches of the GNS-PEG-BDP and GNS-PEG-NH-TR constructs.

Besides thiol exchange, temperature increase over room temperature has been reported to result into thiol desorption from spherical[23,24] and rod-like GNPs.[15]

Biocompatible polyethylene glycols (PEGs), with terminal −SH groups, are very frequently used as coatings for GNPs due to their many advantages in biomedical applications. PEGcoated GNPs display improved pharmacokinetic properties;[25] PEG enhances in vitro stability of GNPs in saline buffers or culture media[25] and it allows the coated nanoparticles to evade macrophage-mediated uptake and removal from systemic circulation in vivo.[11] PEG coating is also employed for nanoparticle specific functionalization, as many commercial PEGs in addition to a thiol function suitable for grafting on gold feature also a remote function (e.g., −OH, −COOH, $-NH_2$) that may be used for further chemical modification.[26,27] GNPs modified with fluorescent dyes are also proposed for biomedical applications as image-enhancing agents[28,29] and as biosensors,[30,31] with the dyes typically grafted to the gold surface through a remote thiol moiety. It must also be added that GNPs have relevant applications in hyperthermal treatments,[2] as when irradiated on their LSPR they undergo thermal relaxation, with a highly localized temperature increase. This is particularly interesting when nonspherical nanoparticles are considered, such as gold nanorods (GNRs)[32] and gold nanostars (GNSs).[33,34] In the latter cases one or two LSPRs are placed in the near-IR range (750−1100 nm), where tissues and blood are semitransparent, so that noninvasive through tissues localized hyperthermal therapies may be envisaged. Recently, photothermally responsive GNSs have been demonstrated to be very efficient in vitro against tumors[35] and bacterial biofilms.[36] In this context the photothermally triggered release of molecular species adhering to GNPs may be considered to be a powerful tool for biomedical applications,[37] as it might offer a synergetic therapeutic effect through the localized drug release in addition to direct local hyperthermal treatments.

On the contrary, the stability of thiol-grafted PEG coatings is typically neglected and taken as assured under all conditions, although under NIR irradiation or even at the temperature typical for in vivo use (36−42 °C) the reviewed literature[15−24] indicates that the S−Au bond is labile and thiols may undergo detachment and displacement by competing species.

On the basis of this background, the study of the lability of thiolate-grafted coatings of photothermally responsive GNSs in aqueous solutions as a function of the temperature and of the nature of codissolved solutes is particularly relevant. To this purpose, we exploited the gold-induced fluorescence quenching of organic dyes that is observed when these are grafted to gold at a short distance.[38−40] The current study was carried out using a model compound, BDP-SH (see Scheme 1), containing the Bodipy fluorophore moiety and a remote thiol group, grafted on GNSs with PEG-SH as the cocoater, as it is shown in Scheme 1B. Bodipy dyes are stable in aqueous solutions and have high fluorescence quantum yields[41] with absorption at 500−530 nm,[42] a range only partially superimposed to the LSPR of GNSs.[34] In the present paper, GNSs were obtained by the well-established lauryl sulfobetaine (LSB)-assisted synthesis.[6,34] These GNSs are mainly pentatwinned branched nanostars (70−80%) (see Scheme 1A), with LSPR tunable in the 750−1100 nm

range[34,36] and centered at ~730−750 nm in the synthetic conditions chosen for this paper. Moreover, it was previously demonstrated that they are photothermally active in aqueous solutions, with specific absorption rate (SAR) as high as 80 kW/g,[33] and with a local increase in temperature at 10 nm from the gold nanostar surface as high as 12 °C.[33] Bodipy fluorescence is strongly quenched by energy transfer to GNPs, while it is recovered when Bodipy is detached and released in solution. We used the recovery of the BDP-SH fluorescence signal as an indicator of the fraction of released dye from GNSs cocoated with BDP-SH and PEG-SH, as it is sketched in Scheme 2B. Temperature variations were studied both by heating GNS solutions with a thermostat and by irradiation of GNSs on their NIR LSPR. Environmental conditions other than temperature were also investigated, such as biological buffers (phosphate-buffered saline (PBS) and RPMI-1640 cell culture broth) and acidic pH values as those found in endosomes, where nano-objects may experience pH values significantly lower than neutral values.[47,48] In parallel, the detachment of PEG-SH under the same conditions was also studied, coating GNSs with an α-thiol-ϖ-amino PEG, targeted on the terminal $-NH_2$ group with the fluorescent tetramethylrhodamine isothiocyanate dye (TRITC), as displayed on Scheme 1C.

[43−46]

Scheme 2. Pictorial Sketch of the Approach Used to Determine the Released BDP-SH (A) and HS-PEG-NH-TR (B) from GNSs[a]

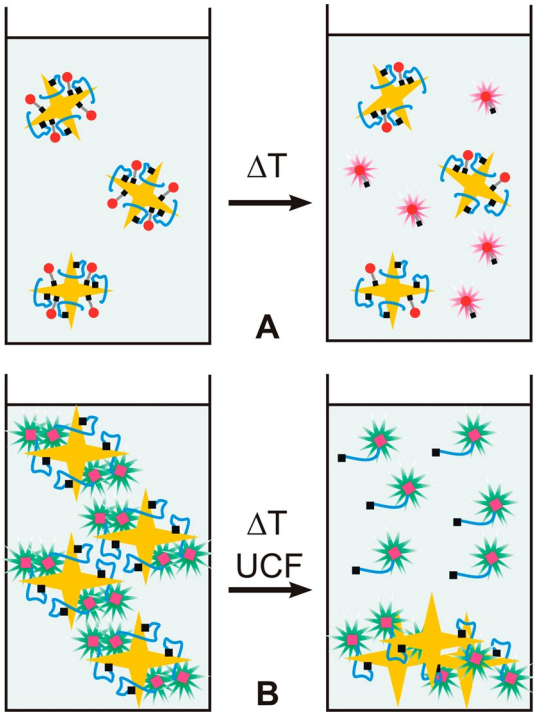

[a]In case A, BDP-SH fluorescence is quenched when it is grafted to GNSs and desorption from GNSs due to T increase is measured by fluorescence revival. In case B, the TR moiety is fluorescent also when HS-PEG-NH-TR is grafted to GNSs. T increase results in HS-PEGNH-TR desorption from GNSs, and after separation from GNSs by ultracentrifugation (UCF) its fluorescence intensity is measured on the supernatant solution.

In this case, the fluorescence moiety is too distant from the gold surface to observe emission quenching when grafted to GNSs, so we adopted a different approach based on supernatant analysis after separation by ultracentrifugation (UCF), as shown in Scheme 2B. As a whole, we obtained a wide picture on the photothermally induced release of surfacebound thiolated drugs and on the stability of thiol coatings in conditions similar to in vivo ones.

2. EXPERIMENTAL SECTION

2.1. Chemicals and GNS Synthesis. Chemicals were purchased from Sigma-Aldrich or Euroclone Cytogenetics and used as received. HS-PEG-NH_2 (mw 3000) was purchased from Rapp Polymere. Additional details can be found in the Supporting Information (SI) (S1.1 Chemicals). BDP-SH was synthesized as previously reported.[42] GNS solutions were obtained by seed growth synthesis with the zwitterionic surfactant LSB, as already described.[6,34] The growth parameters were chosen to obtain the LSPR of the prevalent product (pentatwinned branched GNSs) in the 730−750 nm range.[6,34] Full details of the synthetic protocol are described in the SI (S1.2 GNS Synthesis). After the growth process, GNS solutions were ultracentrifuged, the supernatant discarded, and the GNS pellet was redissolved in the starting volume of bidistilled water and used for further coating.

2.2. Co-Coating of GNSs with PEG-SH and BDP-SH. This was carried out by simultaneously adding 100 μL of 10^{-3} M ethanol solution of BDP-SH and 100 μL of a 10^{-3} M of aqueous solution of PEG-SH to 10 mL of a GNS solution prepared as described in Section 2.1. The concentration of both thiols is thus 1×10^{-5} M. The obtained solution was allowed to equilibrate for 3 h at room temperature while gently shaken on a reciprocating shaker. Excess of PEG-SH and BDPSH was removed by UCF (25 min, 13 000 rpm), followed by supernatant discarding and pellet redissolution in 10 mL of bidistilled water. The cycle was repeated two more times to ensure complete elimination of unbound PEG-SH and BDP-SH. These were our stock solutions, which were stored in the dark at 4 °C. The stock solutions (bound dye concentration is 5.6 ± 0.5 μM) were diluted with bidistilled water or other media in 1:10 ratio for further measurements. Additional details are provided in the SI (S2.1. Co-coating of GNSs with BDP-SH and PEG-SH).

2.3. GNS Coating with HS-PEG-NH_2 and Conjugation with TRITC. This was carried out in two steps. The first step involved the GNS coating with HS-PEG-NH_2 with a procedure analogous to that described in the Section 2.2: 200 μL of a HS-PEG-NH_2 10^{-3} M aqueous solution was added to 10 mL of a GNS solution prepared as described in Section 2.1. Purification from unreacted HS-PEG-NH_2 was obtained by two UCF/redissolution cycles. In the second step, the TRITC dye was conjugated with the grafted bifunctional HS-PEGNH_2 via reaction of the terminal amino group of PEG with the isothiocyanate group of TRITC, leading to the formation of thiourea linkage. 200 μL of 10^{-3} M of TRITC solution (same molar quantity of the HS-PEG-NH_2 added in the previous step) in anhydrous DMF was added to a 10.0 mL solution of GNSs coated with SH-PEG-NH_2, and the obtained solution was kept overnight under gentle stirring on a reciprocating shaker at room temperature. Removal of possible unreacted TRITC was obtained by two UCF/redissolution cycles. Further details are provided in the SI (SI 2.3 GNS Coating with SHPEG-NH_2 and Conjugation with TRITC).

2.4. Spectroscopy Measurements. Absorbance spectra were recorded using a UV/vis/NIR spectrophotometer V-570 (Jasco). The emission spectra were recorded using an Eclipse spectrofluorimeter (Varian, AU). The detector gain (800 V) and the slits size (exc. slit 5 nm; em. slit 10 nm) were kept constant over all measurements. BDPSH was excited at 525 nm, and its maximum emission intensity was observed at 539−541 nm. TRITC dye was excited at 555 nm, and its maximum emission intensity was observed at 578−580 nm.

2.5. Dynamic Light Scattering. Dynamic light scattering (DLS) was performed using a homemade setup described elsewhere.[49] DLS measurements were taken on the solutions before and after the temperature treatments. We investigated the average size and the size distribution for T = 20, 42, and 50 °C (see SI, S9. DLS of the coated with PEG-SH/BDP-SH (ratio 1:1) GNS solutions). The size distributions were computed by applying maximum entropy methods[50,51] to the modulus of the electric field correlation function according to the integral equation described in the SI (S9. DLS of the Coated with PEG-SH/BDP-SH (ratio 1:1) GNS solutions).

2.6. Bulk Temperature Control. For fluorescence studies of BDP-SH and HS-PEG-NH-TR release as a function of the bulk temperature, a 2 mL volume solution of GNS constructs was prepared by diluting 0.2 mL of the stock solutions with 1.8 mL of Milli-Q water. The temperature control was obtained with a Cary temperature controller connected to the Varian spectrofluorimeter.

2.7. Near-Infrared Irradiation. The release of BDP-SH from GNSs was also triggered by irradiating the nanoparticle suspension at λ = 800 nm (Tsunami, Spectra Physics, CA, pulse repetition rate 80 MHz, pulse width 200 fs). The laser was focused on a small volume (30 μL) at the bottom of an Eppendorf tube. Approximately 22 μL was irradiated with average intensity in the range $0.14 \leq \langle I \rangle \leq 2.9$ W/ cm^2, assuming a beam diameter ∼3 mm. The temperature changes were monitored by means of a Thermovision camera (FLIR, USA) with supporting software.

2.8. Quantitative Determination of the Boron Bound on GNSs by Inductively Coupled Plasma Optical Emission Spectroscopy (ICP-OES). A 5 mL sample of GNS solution after the described cocoating procedure was diluted to 10 mL and ultracentrifuged (13 000 rpm, 20 min), the supernatant was discarded, and GNS pellet on the bottom was redissolved in bidistilled water. The procedure was repeated two more times. After the final UCF the supernatant was discarded and the pellet was treated with 1.0 mL of bidistilled water plus 2.0 mL of freshly prepared aqua regia. The blue color of GNSs immediately disappeared and after 24 h the solution was analyzed with ICP-OES using an Optima 3300 DW PerkinElmer instrument.

2.9. Differential Scanning Calorimetry. Differential scanning calorimetry (DSC) experiments were carried out on a Q600 instrument by Thermal Analysis TA on dry pellets of GNSs cocoated with BDP-SH/PEG-SH (1:1 molar ratio in the coating solution) and on GSN coated with HS-PEG-NH_2, both prepared with a 10-fold scaled up preparation. The dry GNSs were obtained after two ultacentrifugation/redissolution cycled by discarding the supernatant after a third UCF and by lyophilizing the wet pellet. DSC measurements were carried out also on pure HS-PEG-NH_2, PEGSH, and BDP-SH, for the sake of comparison. Further experimental details are described in the SI (S.13. DSC and Further Discussion on GNS Coating).

3. RESULTS AND DISCUSSION

3.1. GNSs Cocoated with BDP-SH/PEG-SH. The GNSs used in this paper are prepared according to literature[6,34] and are prevalently pentatwinned branched nanoparticles (TEM images are shown in SI, Figure S4) with LSPR maximum at 730−750 nm. Previous characterization studies[34] showed that these have average branch length of 30 nm with negative zeta potential, ζ potential = −15 mV. Coating was carried out on GNSs by adding a mixture with 1:1 molar ratio BDP-SH/PEGSH. Coating makes the LSPR red shift ∼30 nm (SI, Figure
S3.1.1), as is typical of these GNSs[6,34] when the local refractive index increases due to the surface grafting of molecules less hydrophilic than LSB, like BDP-SH. Typically LSB is completely removed from the surface of these GNSs when adding thiols.[34,53] After the UCF/redissolution purification cycles described in Section 2.2 any trace of LSB was absent (see SI section S.13), as confirmed by DSC. The coated GNSs (species B in Scheme 1) are stable to repeated UCF cycles and are not affected by high NaCl concentration (no spectral changes are observed over 4 h in 0.01 to 1 M NaCl[52]). Their Z potential is −9 mV in pure water and −1 mV in 0.1 M NaCl. Using a 1:1 molar ratio in the coating process, however, does not mean that the two thiols are equimolar also on the GNS surface. It has been shown that the tendency of two competing thiols to graft on an Au surface from the same solution is inversely proportional to their affinity to the solvent.[55−59] Although other interactions (e.g., van der Waals or π stacking) may give a contribution in the monolayer on GNSs, in this case BDP-SH is poorly soluble and PEG-SH is fairly soluble in water, so we should expect a higher surface fraction of the former. We have previously obtained a sharp analysis of the coating composition of this GNS type by DSC on dry GNS samples.[34,53] Unfortunately, although DSC allows us to determine that LSB has been completely removed, GNSs cocoated with BDP-SH and PEG-SH are not stable under the drying and heating procedures. (Spurious peaks are observed when DSC is carried out.) However, we are able to calculate both the concentration and the number of BDP-SH molecules per GNS in our stock solutions: From ICP-OES on GNSs oxidized with acqua regia we obtain boron and gold concentrations. Boron, contained in BDP (see Scheme 1), gives directly the BDP-SH concentration, 5.36×10^{-6} M. Gold is 2.36×10^{-4} M. The average number of BDP-SH molecules per single GNS in the samples, ∼3400, is obtained using the average GNS mass, that we have calculated in a previous paper (5×10^{-17}g/GNS[53]). The cocoated GNSs are resistant to three or more UCF/redissolution cycles, indicating that a consistent quantity of PEG is grafted on their surface. As a further point to support this we carried out preparations with the same total added thiol (BDP-SH + PEG-SH = 2×10^{-6} M) but also with 0.1 to 1.0 BDP-SH: PEG-SH molar fraction in the coating solution. Coated GNSs are stable to three or more UCF cycles only for BDP-SH molar fractions 0.1 to 0.7. Higher molar fractions in the coating solutions give less stable coated GNSs due to the small quantity of grafted PEG-SH. The number of BDP-SH per GNS varies from 2900 to 3600 along the 0.1 to 0.7 molar

fraction series with a linear increase with the BDP-SH molar fraction in the coating mixture, as shown in the SI (Table S2.2.1 and Figure S2.2.1).

GNSs are nonspherical, and one may hypothesize that they have zones in which the coating is more exposed to water (e.g., tips) with respect to other less hydrated zones (e.g., cavities between branches). One may thus also wonder if a preferential disposition of PEG-SH (on tips) and BDP-SH (in cavities) holds, with a "patchy" morphology of the two coaters instead of a random distribution. Vicinal fluorophores, typical of a patchy preferential distribution, may give self-quenching, as it was found on spherical GNPs.[54] It should be expected that the effect is more intense with increasing surface concentration of BDP-SH; however, we examined the fluorescence intensity of the series of GNSs with different BDP-SH molar fractions in the coating solution and found a linear increase with the latter, with no changes in the shape of the emission spectra (SI, Figures S3.2.1 and S3.2.2).

Finally, the concentration of BDP-SH bound to the coated GNSs used in this work (i.e., prepared with 1:1 BDP-SH/PEGSH and used as stock solutions) was calculated also optically. This was done by absorption spectrophotometry, using the BDP-SH extinction coefficient at 525 nm calculated in ethanol ($\varepsilon_{525} = 4.48 \pm 0.2 \times 10^4\ M^{-1}cm^{-1}$) and correcting the absorbance at 525 nm of the coated GNSs by subtracting the contribution of the uncoated GNSs. (Details are shown in the SI section S3.1.) The obtained value is $5.6 \pm 0.5 \times 10^{-6}$ M and in full agreement with the ICP-OES data. This is the concentration of the stock solution used in this paper.

3.2. Estimate of Released BDP-SH as a Function of Bulk Temperature. The fluorescence yield (ratio of the fluorescence emission to the dye concentration) of the grafted BDP-SH as a function of the temperature cannot be measured directly because the dye is released from the GNS surface as the temperature increases. Moreover, the fluorescence yield of free BDP-SH decreases with increasing temperature, as it is shown in the SI (S6. Impact of Temperature and Media on the Intensity of Free and Bound BDP-SH). Therefore, a temperature cycling procedure has been adopted to follow the dye release through the changes of its fluorescence signal, thus circumventing the variations due to the fluorescence yield variation with T. The temperature cycle, shown in Scheme 3, started from the solution at temperature $T_0 = 20$ °C, whose fluorescence is I_0, then a rapid (<30 s) increase in the suspension temperature to $T^{(n)} > T_0$ was obtained where the Scheme 3. Sketch of the Typical Bulk Temperature Cyclic Experiment on the Bodipy-Decorated GNS Solutions[a]

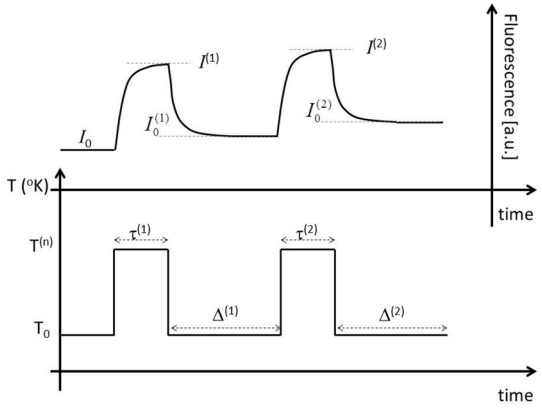

[a] Lower panel reports the temperature kinetics. The transitions between the lower (T_0) and the upper ($T^{(n)}$) temperatures are much shorter than the typical incubation time and are sketched as abrupt changes. The upper panel reports a sketch of the fluorescence emission kinetics both in heating up and in recooling.

fluorescence intensity $I^{(n)}(t)$ was measured for a time stretch $\tau^{(n)}$. The temperature was then rapidly (<30 s) decreased back to T_0, where the fluorescence $I_0^{(n)}(t)$ was followed in time for a time stretch, $\Delta^{(n)}$. The cycles were repeated N times (n = 1, 2, ...N). In this protocol we assumed that all BDP-SH was bound to GNSs before starting the temperature treatment, thus allowing us to calculate the fluorescence yield for the bound fluorophore at 20 °C, $\eta_B(20) = 71.2 \pm 6$ (au). We also assumed that the kinetics of dye regrafting to GNSs occurred on a scale much longer than the cooling time (<30 s): The last assumption was verified experimentally a posteriori. The fluorescence yield of the free fluorophore at 20 °C can be measured on pure BDP-SH, $\eta_F(20) = 2180.8 \pm 4$ (au)

We use a simple relation between the fluorescence emission of samples measured at $T = T_0$ (independent of the heating history of the sample) and the concentration of the BDP-SH released in the suspension ($C_f^{(n)}$)

$$\begin{cases} I_0^{(n)} = \eta_f(20)C_f^{(n)} + \eta_b(20)C_b^{(n)} \\ \quad = [\eta_f(20) - \eta_b(20)]C_f^{(n)} + \eta_b(20)C_{tot} \\ \quad = \Delta\eta_{fb}C_f^{(n)} + I_0 \end{cases} \quad (1)$$

with $C_b^{(n)}$ = concentration of the bound BDP-SH and $C_{tot} = C_b^{(n)} + C_f^{(n)}$. C_{tot} is the concentration of the stock solution diluted 1:10 for the fluorescence experiments, that is, 0.56×10^{-6} M.

An explicit expression for the concentration of the released dye is then obtained as

$$C_f^{(n)} = \frac{I_0^{(n)} - C_{tot}\eta_b(20)}{\Delta\eta_{fb}} = \frac{[I_0^{(n)} - I_0]}{\Delta\eta_{fb}} \quad (2)$$

leading to an expression for the fraction of released dye at the nth step $p^{(n)}_{BD}$ as

$$p_{BD}^{(n)} = C_f^{(n)}/(C_{tot}) \quad (3)$$

The above algorithm does not imply any assumption on the temperature dependence of the fluorescence yield of the bound species.

3.3. Thermal Stability of the Thiol Bonding in Aqueous Media: Single Temperature Jump. The fraction of released BDP-SH from the coated GNSs due to a single exposure at $T^{(1)} > T_0 = 20$ °C for a time lapse in the range 10 min $\leq \tau^{(1)} \leq$ 40 min (see Scheme 3), $p^{(1)}_{BD}$, was investigated by monitoring the BDP-SH emission, and the results are shown in Figure 1A. We always found that after bringing the suspension temperature back to $T_0 = 20$ °C the BDP-SH fluorescence was higher than the preheating value, $I_0^{(1)} > I_0$.

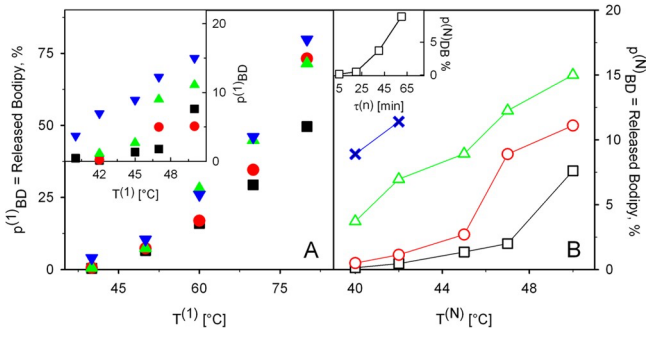

Figure 1. Temperature treatments of GNS-PEG-BDP (prepared with 1:1 molar ratio between thiols in the coating solution) in aqueous solutions. (A) Single-cycle experiments reporting the % fraction of released BDP-SH from coated GNSs as a function of temperature. The symbols refer to incubation times $\tau^{(1)} = \Delta^{(1)} = 5$ (full black squares), 10 (full red circles), 20 (full green up triangles), and 40 min (full blue down triangles). The inset shows a blow up of the region 37 $\leq T^{(1)} \leq$ 50 °C. (B) Repeated (N = 3) temperature cycling experiments showing the influence of temperature ($T^{(n)}$ is the higher temperature of the cycle) and incubation time, $\tau^{(n)}$, on BDP-SH release for $\tau^{(n)} = 5$ (empty black squares), 20 (empty red circles), 40 (empty green triangles), and 60 min (empty blue stars). (Lines are added to guide the eye.) $\Delta^{(n)} = \tau^{(n)}$. The inset reports the released dye fraction (N = 3, $T^{(n)} = 40$ °C) as a function of $\tau^{(n)}$. Data are an average on five experiments, with uncertainties (standard deviations) between ±0.25 and ±0.35%.

This suggests that a fraction of BDP-SH was released at high temperature and was not resorbed on the GNS surface when the suspension was rapidly (within 30 s) brought back at $T = T_0$. By applying eqs 2 and 3, we obtain a fraction of released dye $p^{(1)}_{BD} > 3\%$ only for temperatures above 45 °C, which is, however, outside the physiological range 37−42 °C. It should be noted that a value of 3% is ∼8 times our experimental uncertainty (Figure 1A).

For values of $T^{(1)}$ close to the room temperature and in any case for $T^{(1)} \leq 37$ °C, the thiol bonding in aqueous solutions appears quite stable even for prolonged exposures ($p^{(1)}_{BD} \leq$ 4% for $T^{(1)} < 40$ °C and $\tau^{(1)} \leq 40'$, Figure 1A).

3.4. Thermal Stability of the Thiol Bonding under Temperature Cycling. As shown in Section 3.3, below $T^{(1)} =$ 50 °C the effect of the incubation time on $p^{(1)}_{BD}$ appears only for long heating times. Nevertheless, understanding the release trend at temperatures below 50 °C is essential for biomedical application, in which prolonged and repeated photothermal treatments could be carried out with the same GNS batch. Accordingly, we tried to increase the released dye fraction in the range 40 $\leq T^{(n)} \leq$ 50 °C by performing repeated (N = 3) cycles $(20 \rightarrow T^{(n)} \rightarrow 20\ °C)_{n=1,...N}$ with different incubation times $\tau^{(n)}$ and $\Delta^{(n)} = \tau^{(n)}$ (Figure 1B). The fraction of released dye was computed according to eq 3 from the fluorescence intensity, $I^{(N)}_0$ (see Scheme 3), measured after the suspension was recooled to room temperature, T_0, after the last heating cycle.

As it can be seen from Figure 1B, incubation times from $\tau^n = 5$ min to $\tau^n = 20$ min did not significantly impact the release of BDP-SH in the range 40−45 °C ($p_{BD} < 2.5\%$); however, for $\tau^n = 40$ min or above, the fraction of released dye rose to 9−11% at $T^{(3)} = 40 - 42$ °C (Figure 1B, stars). The released dye fraction increased nonlinearly with the incubation time (Figure 1B, inset). Moreover, it was found that the reduction of the relaxation time at 20 °C to $\Delta^{(n)} \approx 4$ to 5 min $\leq \tau^{(n)}$, while performing these cycles led to an increase in the fractions of released BDP-SH. At $T^{(n)} = 40$ °C, the BDP-SH released fraction of ∼5% ($\Delta^{(n)} = 5$ min, $\tau^{(n)} = 40$ min) was reached and this value raised to ∼15% for cycling at $T^{(n)} = 50$ °C.

3.5. Full BDP-SH Release from GNSs at $T^{(n)} = 80$ °C. In the previous analysis we relied on the assumption that BDP-SH was initially completely bound to gold nanostars in our GNSPEG-BDP solutions. The degree of approximation of this assumption was verified by performing repeated (N = 15) cycles $T^0 \rightarrow T^{(n)} \rightarrow T^0$ at a very high temperature, $T^{(n)} \approx 80$ °C, for intermediate values of incubation times $\tau^{(n)} = 10$ min and $\Delta^{(n)} = 10$ min. We reasoned that in this way we should be able to reach complete release of BDP-SH bound to the gold nanostars. The concentration of the dye obtained by eq 3 was compared with the values obtained from the absorption spectrum of the GNS-PEG-BDP construct under the assumption that the dye extinction coefficient was not significantly affected by the vicinity of the GNP surface. The values of intensity, $I^{(n)}_0$, measured at the end of each of the $\Delta^{(n)} = 10$ min incubation periods at $T = 20$ °C, are reported in Figure 2A (blue squares) and display an overall exponential growth that can be fitted according to $I_0^{(n)}(t) = I_\infty - \Delta I^{(t/t_{rel})}$. From a single exponential fit (solid line) we obtain $t_{rel} \approx 60$ min for $T = T_0$.

We also followed the change in Bodipy emission during a single long-lasting incubation at high temperature $T^{(1)} = 80$ °C. The fluorescence intensity increase could be analyzed as a single exponential growth with relaxation time t_{rel} =48 ± 4 min (Figure 2A, inset) smaller than that measured under alternated heating $t_{rel} \approx 60$ min ($T = T_0$) (Figure 2A, squares). This result can be explained as a partial resorption of the dye to the gold surface in each low-temperature interval.

It has to be stressed that the final lower value of $I_0^{(n)}$ in the single cycle release at 80 °C (inset, red circles, $I_0^{(n)}$ measured at 80 °C) with respect to repeating heating cycles (panel A, blue squares, $I_0^{(n)}$ measured at 20 °C) is due to the intrinsic lower emission intensity of BDP-SH at higher temperatures. (Details are provided in the SI, section S6.). The fraction of dye released in the solution, $p^{(BD^n)}$, obtained from the data reported in Figure 2, closely approached 100% (99% ± 0.2, for $\tau^{(n)} = 10$ min, N = 15), and the value was independent of the incubation time $\tau^{(n)}$ from 10 to 60 min (97 ± 0.5%, for $\tau^{(n)} = 60'$, N = 1). These results confirm the validity of the assumption for the derivation of eq 1 stating that all (99%) of the dye was bound to the GNS surface before starting the thermal treatment and provide the value of bound BDP-SH concentration = 5.6 ± 0.5 μM in stock solutions.

3.6. PEG-SH Release Induced by Temperature. Although the structure, bulkiness, and hydrophilicity of the appended groups are very different for PEG-SH and BDP-SH,

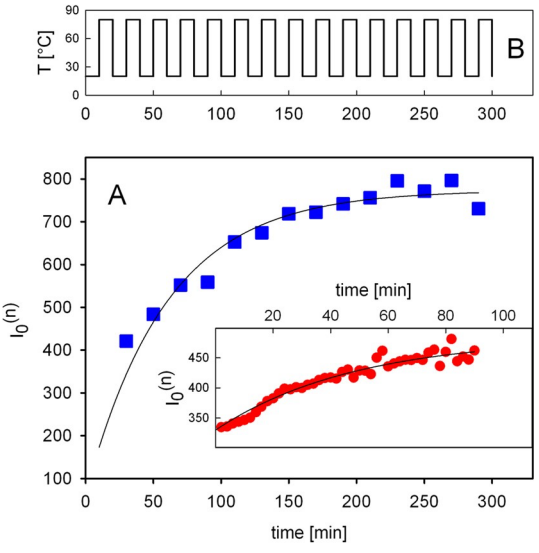

Figure 2. Kinetics of the Bodipy fluorescence emission in water under repeated heating cycles with n = 1, 2, ...15 and $T^{(n)} = 80$ °C. (A) Bodipy fluorescence at the end of each incubation period at $T_0 = 20$ °C ($I_0^{(n)}$, blue squares). The solid line is the best fit to a single exponential growth function. Inset: fluorescence kinetics after bringing the GNS-PEG-BDP suspension at $T^{(1)} = 80$ °C (red circles, single cycle experiment, $\tau^{(1)} = 90$ min). The solid lines are the best-fit singleexponential growth function to the data. (B) Diagram of the temperature in the solution. All GNSs prepared with 1:1 molar ratio between thiols in the coating solution.

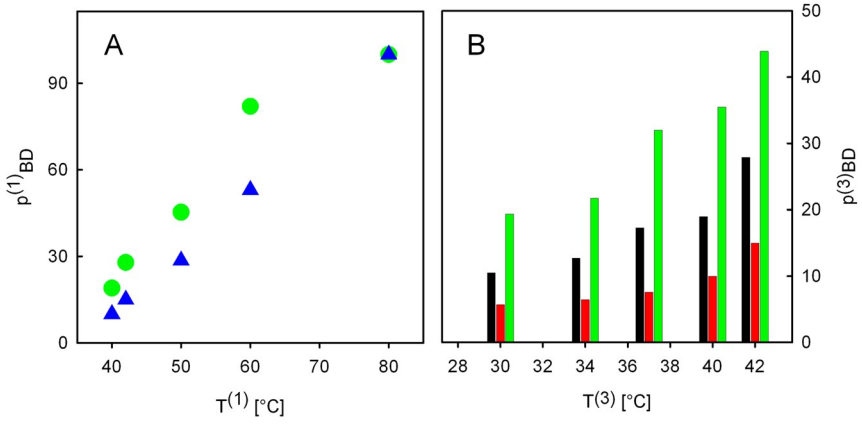

Figure 3. (A) Release of Bodipy in aqueous (blue triangles) and in PBS solutions (green circles) in the range $40 \le T^{(n)} \le 80$ °C for a single step cycle. (B) Fraction of released dye measured for a three-step cycle (N = 3) in the temperature range 30−42 °C for aqueous (red bars), PBS stock (black bars), and RPMI (green bars). All GSN prepared with 1:1 molar ratio between thiols in the coating solution.

they are both terminated with a $-CH_2-CH_2-SH$ moiety, as shown in Scheme 1. Accordingly, the nature and the energy of the S−Au bond are expected to be similar between them, and a fraction of the grafted PEG-SH could may be as well desorbed on increasing temperature. Being that PEG-SH is colorless and nonfluorescent, the release of the PEG thiol was studied with a different approach, illustrated by Scheme 2B. A bifunctional HS-PEG-NH_2 was used, and its free primary amino groups were labeled with the TRITC dye (see species C, Scheme 1) via the isothiocyanate-amine coupling

reaction, which leads to the formation of the thiourea linkage shown in Scheme 1. The shorter HS-PEG-NH_2 polymer available from our suppliers has mw =3000, while the PEG-SH polymer used for cocoating with BPD-SH has mw = 2000. This makes the two molecules very similar and comparable although not strictly identical. DSC measurements sharply evidenced the full elimination of LSB from GNS surface and allowed us to calculate that HS-PEGNH_2 is the 7.5% weight of the coated GNSs (SI section S13) corresponding to 810 molecules per GNS, in very good agreement with the 780 PEG chains per GNS found when using PEG-SH with mw 2000.[53] Also, in this case, we checked the stability of GSN coated with HS-PEG-NH_2 using high NaCl concentration, and no spectral changes were observed over 4 h in 0.01 to 1 M NaCl.[52] TRITC conjugation was carried out with an excess TRITC with respect to the HS-PEG-NH_2 grafted on the GNSs, and this is expected to yield the allfunctionalized GNS-PEG-NH-TR constructs pictorially described by structure C in Scheme 2. (See also SI, section S.14, for experimental evidence.) TRITC fluorescence has a maximum of emission (λ_{em}) at 580 nm. Because of the long PEG spacer, TRITC dye is not kept near the gold surface as the Bodipy moiety in BDP-SH; therefore, the fluorescence emission of TRITC is not quenched (as shown in the cartoon on the left of Scheme 2B). The release of TRITC-labeled PEG chains was then studied by temperature cycles, followed by UCF to separate the released labeled PEG from the GNS suspension (remaining in the supernatant, cartoon on the right of Scheme 2B). The concentration of starting and released PEG is then determined by fluorimetry. Details of this procedure are described in the SI (Section S10). The results of this analysis show that, during the thermal treatment of the GNS solutions, PEG-SH chains are also released from the surface of GNSs. The fraction of released PEG was ∼16% at $T^{(1)}$ = 37 °C and raised to ∼20% for $T^{(1)}$ = 42 °C for incubation time $\tau^{(1)}$ = 60 min. Similarly to the experiments aimed at the BDP-SH release, repeated (N = 3) thermal treatments at high temperature $T^{(n)}$ = 80 °C, $\tau^{(n)}$ = 60′, led to the full release of PEG from the GNSs. We must stress that for this analysis GNSs were fully coated with a single bifunctional, labeled PEG, a condition different from the GNS-PEG-BDP constructs prepared with a BDPSH:PEG-SH 1:1 mixed coating solution. Also (see Scheme 1), we have already mentioned that the bifunctional PEG used in this section has a longer chain than the PEG-SH used for cocoating with BDP-SH. Consequently the % of released TRlabeled PEG chains from GNS-PEG-NH-TR should not be assumed as the % of released PEG-SH from the mixed-coated species GSN-PEG-BDP; however, focusing on the gold−PEG interaction, the two PEG-thiols are identical up to a distance of 44 (CH_2−CH_2−O−) units from the Au surface. It can thus be considered to be significant data that the fraction of released PEG found here is larger than that of BPD-SH. Moreover, this is not surprising because it is in agreement with the common observation that the competitive deposition of two different thiols, R′-SH and R″-SH, on gold surfaces depends mainly on the differences in the solvent affinity (solubility) of the R′ and R″ moieties.[55−57] The lower fraction on the surface is found for the most soluble species in the chosen solvent. In the case of GNS-PEG-BDP we deal with the reverse process (release of R′SH and R″-SH from a mixed surface) but we may reasonably expect that the thiol with the highest affinity toward water is more easily released. While BDP-SH is poorly water-soluble, any PEG polymer is highly soluble in aqueous solutions.

3.7. Temperature-Induced Aggregation. Because the previous sections show that a small but significant fraction of both BPD-SH and PEG-SH are released even with small temperature increase, we investigated the effect of temperature also on the aggregation of GNSs by DLS. The initial (at $T = T_0 = 20$ °C) distribution of the GNS size depends on the typical features of the synthesis. (See the SI for details, section S9.) We always found a major, narrow, component (at least 75% in amplitude) with $d_H = 110 \pm 28$ nm (Figure S9.1 in the SI, solid line). This average value was computed as the z average over the major component of the distribution $d_H = 2R_H$, as described in the SI (S9. DLS of the Coated with PEG-SH/BDP-SH (ratio 1:1) GNS Solutions). During the temperature cycles ($T^{(n)}$= 42 °C) the size distribution shifts to larger sizes and widens. (See Figures S9.1 and S9.2A in the SI.) It must be noticed that eventually, after N = 3−5 cycles, we recover at $T = T_0$ a single dominant component of intermediate size $30 \le d_H \le 200$ nm with at most some tiny contributions for $d_H > 1$ μm. (See also Table S9.1 in the SI.) In all cases the fraction of nonaggregated GNSs (SI and Figure S9.1, inset) is 75 ± 15% for $\Delta^{(n)}$ = 5 min and lowers to small values (∼10%) only when the incubation time is longer than $\tau^{(n)}$ = 40 min. The BDP-SH and PEG-SH release from the Au surface could be responsible for this minor nanoparticle aggregation after temperature treatments. This may also affect the kinetics of resorption of the dye onto the gold surface.

3.8. Effect of Medium Chemical Composition and pH on BDP-SH Release. For biomedical or biotechnological application coated gold nanostars are diluted in biological fluids, containing salts and proteins that may also effect on the stability of the thiol bonding. Therefore, purposely to investigate the role of the medium composition, single temperature jumps and temperature cycles were carried out on GNSs cocoated with 1:1 PEG-SH and BDP-SH and dissolved in PBS (stock and 1% solutions), RPMI media, and acidic buffer. The used $T^{(n)}$, $\Delta^{(n)}$, and $\tau^{(n)}$ parameters were chosen as described for the pure water experiments (Sections 3.3 and 3.4). Although in vivo the formation of "corona" due the nanoparticles interaction with a range of biomolecules should be taken into account, the biological fluids investigated here cover at least a wide range of properties. PBS, a buffer frequently used in biological applications especially for preliminary researches in vitro, is an aqueous saline solution at pH 7.4 based on sodium and potassium chloride and hydrogen phosphate (chloride concentration ca. 0.15 M) without magnesium or calcium. RPMI-1640 cell media is widely applied for supporting the growth of many types of cultured cells, and it contains amino acids and high

concentrations of vitamins and salts. The fraction of BDP-SH released in these media was computed from the fluorescence emission of the solutions after they were recooled at T_0 = 20 °C according to eqs 2 and 3. A significantly larger temperatureinduced dye release was measured in PBS solutions (green circles, Figure 3A) with respect to what was observed in pure aqueous solutions (blue triangles, Figure 3A). Repeated temperature cycles (N = 3, $\tau^{(n)}$ = 40 min; $\Delta^{(n)}$ = 5 min) were then performed for $T^{(n)}$ = 30, 34, 37, 40, and 42 °C in PBS and RPMI media and compared with pure water. The results, shown in Figure 3B, indicated that the largest dye release was obtained in RPMI (~40% dye release at $T^{(n)}$ = 42 °C), although also PBS media enhances BDP-SH release (~30% dye release at $T^{(n)}$ = 42 °C), compared with the poor release of BDP-SH in pure aqueous medium.

The media composition also affects the kinetics of the desorption and resorption of BDP-SH from GNSs, which is valuable information for pharmacological treatments. After a complete dye release reached by exposing the GNS solutions at $T^{(1)}$ = 80 °C (N = 1), we monitored by means of fluorescence decay the spontaneous resorption of the dye occurring when recooling the suspension to T_0 = 20 °C. The measured kinetics can be described by a single exponential component = exp[−t/ τ_{rel}], as shown in SI (S7. Kinetics of Dye Resorption after Full Release, Figure S7.1 in the SI) with very long relaxation times. For the aqueous and PBS solutions t_{rel} was ~120 h.

Finally, because the intracellular environment is mainly acidic,[47] we also monitored the BDP-SH emission intensity in

acidic media during temperature treatments. Mild cycles (T_0 =20 °C; $T^{(n)}$ = 42 °C; $\tau^{(n)}$ = 40 min, N = 3) were performed in acidic buffer at pH 4.2, and we measured BDP-SH release up to 40% (Table S6.6 in the SI). Moreover, after the release of the dye in acidic medium the emission intensity of dye decreased dramatically due to degradation of the Bodipy moiety in this medium.[58] This fact was additionally verified by performing the same cycles with solutions of free BDP-SH (see SI, Tables S6). For times longer than 40 min no substantial increase in the

BDP-SH release could be detected. (See Table S6.6 in the SI.)

3.9. Near-Infrared Irradiation of GNS-PEG-BDP Constructs. We have studied the release of BDP-SH from the GNS-PEG-BDP constructs induced by the irradiation of the solutions with NIR laser radiation tuned at λ = 800 nm, that is, within the LSPR of these GNSs (Figure S3.1.1 in the SI). We assumed that the release was an indirect effect of the LSPR absorption by the GNSs, that thermally relax, resulting in a temperature increase in the solution.[34,59] It must be pointed out that the temperature on the surface of these GNSs, when laser irradiated, is only slightly higher (10%) than the temperature of the bulk suspension[33] (with this difference disappearing within 6.5−8.5 nm from the GNS surface), allowing us to measure and use the bulk suspension temperature as the parameter that determines the BDP-SH release. Accordingly, we have first investigated the effect of the laser intensity and of the nanoparticle concentration on the suspension temperature using 20-fold concentrated GNS solutions with respect to stock solutions. The temperature was found to increase versus time with a double exponential trend up to a plateau value (Figure 4). The slower relaxation component can be ascribed to the exchange of the solution with the laboratory environment, on the order of 150−500 s (see the SI, section S12), and accounts for at least half of the overall temperature increase. (See Figure 4 and Figure S12.1 in the SI.) The faster component can be ascribed to the heat exchange within the irradiated suspension.[59] The overall increase in the suspension temper-

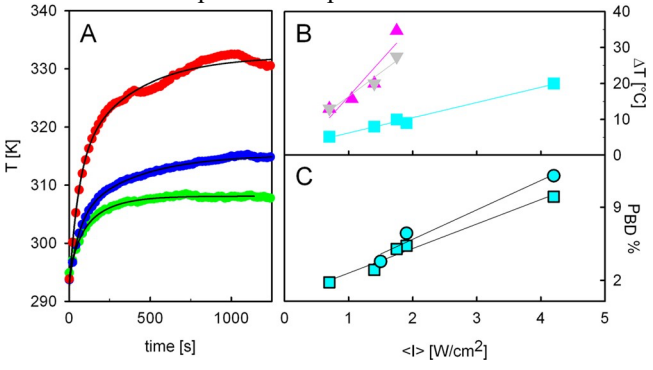

Figure 4. (A) NIR-induced temperature increase in GNS-PEG-BDP solutions. Symbols refer to NIR intensities <I> = 0.7 (green circles), 1.4 (blue circles) and 1.8 (red circles) W/cm^2. Solid lines are data best fits to the function $T_\infty - \Delta T_{fast} \exp(-t/\tau_{fast}) - \Delta T_{slow} \exp(-t/\tau_{slow})$. The GNS concentration was C = 0.78 mg/mL. (B) Solution temperature increase for C = 0.39 (cyan squares), 0.78 (gray down triangles), and 1.95 mg/mL (purple up triangles). Lines are linear best fits with slopes: 17 ± 2 [°C·cm^2/W] (C = 1.95 mg/mL), 15 ± 2 [°C· cm^2/W] (C = 0.78 mg/mL) and 5 ± 0.2 [°C·cm^2/W] (C = 0.39 mg/ mL). (C) Fraction of released Bodipy as a function of <I> for treatment duration $\tau^{(1)}$ = 40 min (cyan squares) and $\tau^{(1)}$ = 60 min (cyan circles; C = 0.39 mg/mL). The lines are linear best fits with slopes: 2.4 ± 0.1 [cm^2/W] ($\tau^{(1)}$ = 40 min) and 2.8 ± 0.2 [cm^2/W] ($\tau^{(1)}$ = 60 min). GNSs prepared with 1:1 molar ratio between thiols in the coating solution.

ature has a linear dependence on the irradiation intensity <I>; however, we observed a reduced dependence of the temperature increase in the GNS concentration (Figure 4B): the slope $\partial\Delta T/\partial$<I> changes from 5 ± 0.2 [°C·cm^2/W] for C = 0.39 mg/mL to 15 ± 2 [°C·cm^2/W] for C = 0.78 mg/mL and does not substantially increase upon raising the concentration to C = 1.95 mg/mL ($\partial\Delta T/\partial$<I> = 17 ± 0.2 [°C·cm^2/W]). This is likely due to the overall extinction (scattering and absorption) of the NIR radiation by the nanoparticles with a reduction of the effective radiation that can be absorbed by the GNSs.

Because of the high concentration of GNSs in the concentrated samples it was also impossible to collect the fluorescence emitted by the released dye. Therefore, the sample was centrifuged (10 min, 13 000 rpm) immediately after the NIR irradiation and the emission and excitation

spectra of the supernatant were recorded. As a control we measured the emission of the supernatant of a nonirradiated GNS-PEG-BDP solution, finding negligible dye emission (λ_{em} = 540 nm). Because the concentration of dye in these samples was too low to allow an accurate measurement of the supernatant absorbance, we have exploited the much more sensitive fluorescence signal. To quantify the released BDP-SH concentration we calibrated the emission and excitation spectra intensity as a function of free BDP-SH concentration as described in the SI (Section S11). The percentage of the released BDP-SH obtained in this way is summarized in Figure 4C. The released fraction increases linearly with the irradiation <I> (Figure 4C) and correlates with irradiation time (Figure 4C). This finding proves the origin of NIR-activated release. The amount of released dye is <13%, even at <I> = 4.2 [W/ cm^2] and with long irradiation times (60 min). The 20% increase in the slope, $\partial P^{\%}_{BD}/\partial <I>$ from 2.4 ± 0.1 [cm^2/W] for irradiation time $\tau^{(1)}$ = 40 min to 2.9 ± 0.2 [cm^2/W] for $\tau^{(1)}$ = 60 min observed in Figure 4C, does not reflect the 50% increase in the irradiation times due to the saturation time of the temperature increase, which is on the order of 5−10 min. (See Figure 4A and Table S12.1 in the SI.)

4. CONCLUSIONS

In this work the stability of thiol bonding on the surface of GNPs in aqueous solutions and biologically relevant conditions was studied as a function of temperature and solution composition. We used GNSs cocoated with the fluorescent dye BDP-SH and PEG-SH, a construct that is representative of nanotools that could be used simultaneously for photothermal treatments and drug delivery. It must be stressed that most of the literature regards the use of thiol-coated spherical GNPs and we have used here star-shaped GNPs. Moreover, the PEGSH used for cocoating has mw 2000, and shorter or longer PEG chains may bury and hide to a different extent the BDP-SH molecules on the GNS surface (influencing its release kinetics): so some caution should be used on generalizing these results; however, we have evidenced a clear effect of temperature that decreases the stability of the thiol bonding even in the narrow physiological range 37−42 °C. Investigation of the kinetics of desorption and resorption of the BDP-SH to the GNS surface also evidenced that repeated cycling between two temperatures leads to a larger release of the dye from the GNS surface with respect to a single, prolonged, thermal treatment. Moreover, we have evidenced that between the poorly hydrophilic BDP-SH and the strongly hydrophilic PEG-SH the latter is released in a larger fraction from the GNS surface, consistently with its higher affinity for the solvent. It is even more relevant that the salt, amino acid, and vitamin content of the suspending solution have an important detrimental effect on the thiol bonding stability, larger than the pure thermal effect. All of these results indicate that the bond between the gold surface and commercial PEG polymers bearing a single −SH function may not be as inert as it is commonly considered, suggesting the need of a careful control of the stability of thiol protective coatings in biological environments, especially when they are to be used in vivo for prolonged times and for photothermal applications. Copolymers bearing PEG chains and featuring multiple thiol or disulfide functions may be the obvious answer to these drawbacks[60] because they offer all of the useful properties of PEG and the enormously increased grafting stability due to surface−polymer multipoint interactions. On the contrary, especially in the case of hydrophyilic drugs bound with a single thiol to GNP, our work indicates that a phothermally induced local increase in temperature may be an efficient tool to obtain switchable drug release.

ASSOCIATED CONTENT

* Supporting Information

Additional data about experimental details; kinetics of BDP-SH and PEG-SH release from GNSs under bulk temperature increase; impact of temperatures and media on the emission intensity of solutions of free and bound dye; long-term kinetics of BDP-SH resorption after full release in aqueous media and PBS solutions; temperature-activated full release of BDP-SH from GNSs; DLS measurements; calibration plots of the emission and excitation spectra as a function of free BDP-SH concentration; NIR irradiation data; and DSC data; ^{1}H NMR data. The Supporting Information is available free of charge on the ACS Publications website at DOI: 10.1021/acs.langmuir.5b01473.

AUTHOR INFORMATION

Corresponding Authors

*E-mail: mykola.borzenkov@unimib.it (M.B.).

*E-mail: piersandro.pallavicini@unipv.it (P.P.).

Author Contributions

The manuscript was written through contributions of all authors. All authors have given approval to the final version of the manuscript.

Notes

The authors declare no competing financial interest.

ACKNOWLEDGMENTS

We acknowledge the funding of Fondazione Cariplo, grant no. 2010-0454 and MIUR (PRIN 2010-2011, 20109P1MH2_003). We are grateful to Sara Perotto for assistance in NIR irradiation experiments.

REFERENCES

(1) Sperling, R. A.; Pilar, R.; Zhang, F.; Zanella, M.; Parak, W. J. Biological application of gold nanoparticles. Chem. Soc. Rev. 2008, 37, 1896−1908.

(2) Huang, X. H.; Jain, P. K.; El-Sayed, I. H.; El-Sayed, M. A. Plasmonic photothermal therapy (PPTT) using gold nanoparticles. Lasers Med. Sci. 2008, 23, 217−228.

(3) Anwar, M. K.; Jarrar, B. M. Histological alterations in the liver of rats induced by different gold nanoparticles sizes, doses and exposure durations. J. Nanobiotechnol. 2012, 10, 5−13.
(4) Daniel, M.; Astruc, D. Gold nanoparticles: assembly, supramolecular chemistry, quantum-size-related properties, and applications toward biology, catalysis, and nanotechnology. Chem. Rev. 2004, 104, 293−346.
(5) Anker, N. J.; Hall, P. W.; Lyandres, O.; Shah, N. C.; Zhao, J.; Van Duyne, R. P. Biosensing with plasmonic nanosensors. Nat. Mater. 2008, 7, 442−453.
(6) Pallavicini, P.; Chirico, G.; Collini, M.; Dacarro, G.; Dona, A.; D′Alfonso, L.; Falqui, A.; Diaz-Fernandez, Y.; Freddi, S.; Garofalo, B.; Genovese, A.; Sironi, L.; Taglietti, A. Synthesis of branched Au nanoparticles with tunable near-infrared LSPR using a zwitterionic surfactant. Chem. Commun. 2011, 47, 1315−1317.
(7) Huang, H. S.; Hainfeld, J. F. Intravenous magnetic nanoparticles cancer hyperthermia. Int. J. Nanomed. 2013, 8, 2521−2532.
(8) Sperling, R. A.; Parak, W. J. Surface modification, functionalization and bioconjugation of colloidal inorganic nanoparticles. Philos. Trans. R. Soc., A 2010, 368, 1333−1383.
(9) Zeng, S.; Yong, K.-T.; Roy, I.; Dinh, X.-Q.; Yu, X.; Luan, F. A review on functionalized gold nanoparticles for biosensing applications. Plasmonics 2011, 6, 491−506.
(10) Han, G.; Ghosh, P.; Rotello, V. M. Multi-Functonal Gold Nanoparticles for Drug Delivery. In Bio-Applications of nanoparticles; Warren, C. W., Ed.; Springer Science: New York, 2007; pp 48−56.
(11) Sanna, V.; Pala, N.; Sechi, M. Targeted therapy using nanotechnology: focus on cancer. Int. J. Nanomed. 2014, 9, 467−483. (12) Dykman, L. A.; Khlebstov, N. G. Gold nanoparticles in biology and medicine: recent advances and prospects. Chem. Soc. Rev. 2011, 3, 32−55.
(13) Gronbeck, H.; Curioni, A.; Andreoni, W. Thiols and disulfides on Au (III) surface: the headgroup-gold interaction. J. Am. Chem. Soc. 2000, 122, 3839−3842.
(14) Nuzzo, R. G.; Dubois, L. H.; Allara, D. L. Fundamental studies of microscopic wetting on organic surfaces. 1. Formation and structural characterization of a self-consistent series of polyfunctional organic monolayers. J. Am. Chem. Soc. 1990, 112, 558−569.
(15) Gustafson, T. P.; Cao, Q.; Wang, S. T.; Berezin, M. Y. Design of irreversible optical nanothermometers for thermal ablations. Chem. Commun. 2013, 49, 680−682.
(16) Ito, E.; Kang, H.; Lee, D.; Park, J. B.; Hara, M.; Noh, J. Spontaneous desorption and phase transitions of self-assembled alkanethiol and alicyclic thiol monolayers chemisorbed on Au(1 1 1) in ultrahigh vacuum at room temperature. J. Colloid Interface Sci. 2013, 394, 522−529.
(17) Bain, C. D.; Troughton, E. B.; Tao, Y.-T.; Evall, J.; Whitesides, G. M.; Nuzzo, R. G. Formation of Monolayer Films by the Spontaneous Assembly of Organic Thiols from Solution onto Gold. J. Am. Chem. Soc. 1989, 111, 321−335.
(18) Maciel, J.; Martins, M. C. L.; Barbosa, M. A. The stability of selfassembled monolayers with time and under biological conditions. J. Biomed. Mater. Res., Part A 2010, 94A, 833−843.
(19) Mani, G.; Johnson, D. M.; Marton, D.; Dougherty, V. L.; Feldman, M. D.; Patel, D.; Ayon, A. A.; Agrawal, C. M. Stability of selfassembled monolayers on titanium and gold. Langmuir 2008, 24, 6774−6784.
(20) Hostetler, M. J.; Templeton, A. C.; Murray, R. W. Dynamics of place-exchange reactions on monolayer-protected gold cluster molecules. Langmuir 1999, 15, 3782−3789.
(21) Song, Y.; Murray, R. W. Dynamics and extent of ligand exchange depend on electronic charge of metal nanoparticles. J. Am. Chem. Soc. 2002, 124, 7096−7102.
(22) Haller, E.; Stubiger, G.; Lafitte, D.; Lindner, W.; Lammerhofer, M. Chemical Recognition of Oxidation-Specific Epitopes in LowDensity Lipoproteins by a Nanoparticle Based Concept for Trapping,Enrichment, and Liquid Chromatography−Tandem MassSpectrometry Analysis of Oxidative Stress Biomarkers. Anal. Chem. 2013, 49, 680−682.
(23) Bhatt, N.; Huang, P. J.; Dave, N.; Liu, J. Dissociation and degradation of thiol-modified DNA on gold nanoparticles in aqueous and organic solvents. Langmuir 2011, 27, 6132−6137.
(24) Zandberg, W. F.; Bakhtiari, A. B. S.; Erno, Z.; Hsiao, D.; Gates, B. D.; Claydon, T.; Branda, N. R. Photothermal release of small molecules from gold nanoparticles in live cells. Nanomedicine 2012, 8, 908−915.
(25) Rahme, K.; Chen, L.; Hobbs, R. G.; Morris, M. A.; O′Driscoll, C.; Holmes, J. D. PEGylated gold nanoparticles: polymer quantification as a function of PEG lengths and nanoparticles dimensions. RSC Adv. 2013, 3, 6085−6094.
(26) Manson, J.; Kumar, D.; Meenan, B. J.; Dixon, D. Polyethylene glycol functionalized gold nanoparticles: the influence of capping density on stability in various media. Gold Bull. 2011, 44, 99−105.
(27) Kumar, R.; Korideck, H.; Ngwa, W.; Berbeco, R. I.; Makrigiorgos, G. M.; Sridhar, S. Third generation gold nanoplatform optimized for radiation therapy. Transl. Cancer Res. 2013, 4, 228−239. (28) Shenoi, M. M.; Iltis, I.; Jeunghwan, C.; Koonce, N. A.; Metzger, G. J.; Griffin, R. J.; Bischof, J. C. Nanoparticles delivered vascular distributing agents (VDAs): Use of TNF-alpha conjugated gold nanoparticles for multimodal cancer therapy. Mol. Pharmaceutics 2013, 10, 1683−1694.
(29) Oishi, M.; Nakamura, T.; Jinji, Y.; Matsuishi, K.; Nagasaki, Y. Multi-stimuli-triggered release of charged dye from smart PEGylated nanogels containing gold nanoparticles to regulate fluorescence signals. J. Mater. Chem. 2009, 19, 5909−5912.
(30) Sironi, L.; Freddi, S.; D′Alfonso, L.; Collini, M.; Gorletta, T.; Soddu, S.; Chirico, G. Detection by fluorescence lifetime on a hybrid fluorescein isothiocyanate gold nanosensor. J. Biomed. Nanotechnol. 2009, 5, 683−691.
(31) Zhang, J.; Lio, B.; Liu, H.; Zhang, X.; Tan, W. Aptamer − conjugated gold nanoparticles for bioanalysis. Nanomedicine 2013, 8, 983−993.
(32) Huff, T. B.; Tong, L.; Zhao, Y.; Hansen, M. N.; Cheng, J. X.; Wei, A. Hyperthermic effects of gold nanorods on tumor cells. Nanomedicine 2007, 2, 125−132.
(33) Freddi, S.; Sironi, L.; D′Antuono, R.; Morone, D.; Dona, A.; Cabrini, E.; D′Alfonso, L.; Collini, M.; Pallavicini, P.; Baldi, G.; Maggioni, D.; Chirico, G. A molecular thermometer for nanoparticles for optical hyperthermia. Nano Lett. 2013, 13, 2004−2010.
(34) Casu, A.; Cabrini, E.; Dona, A.; Falqui, A.; Diaz-Fernandez, Y.; Milanese, C.; Taglietti, A.; Pallavicini, P.

Controlled synthesis of gold nanostars using a zwitterionic surfactant. Chem. - Eur. J. 2012, 18, 9381−9390.

(35) Yuan, H.; Fales, A. M.; Vo-Dinh, T. TAT Peptide-Functionalized Gold Nanostars: Enhanced Intracellular Delivery and Efficient NIR Photothermal Therapy Using Ultralow Irradiance. J. Am. Chem. Soc. 2012, 134, 11358−11361.

(36) Pallavicini, P.; Dona, A.; Taglietti, A.; Minzioni, P.; Patrini, M.; Dacarro, G.; Chirico, G.; Sironi, L.; Bloise, N.; Visai, L.; Scarabelli, L. Self-assembled monolayers of gold nanostars: a convenient tool for near-IR photothermal biofilm eradication. Chem. Commun. 2014, 50, 1969−1971.

(37) Voliani, V.; Signore, G.; Nifosi, R.; Rici, F.; Luin, S.; Beltram, F. Smart delivery and controlled drug release with gold nanoparticles: new frountiers in nanomedecine. Recent Pat. Nanomed. 2012, 2, 34−
44.

(38) Yang, P. J.; Chu, H.; Lee, Y.; Kobayashi, T.; Chen, T.; Lin, H.-C. Quenching effects of gold nanoparticles in nanocomposites formed in water-soluble conjugated polymer nanoreactors. Polymer 2012, 53, 939−946.

(39) Dulkeith, E.; Ringler, M.; Klar, T. A.; Feldmann, J.; Muñoz Javier, A. M.; Parak, W. J. Gold nanoparticles quench fluorescence by phase induced radiative rate suppression. Nano Lett. 2005, 5, 585−589. (40) Anger, P.; Bharadwaj, P.; Novotny, L. Enhancement and quenching of single-molecule fluorescence. Phys. Rev. Lett. 2006, 96, 113002.

(41) Thivierge, C.; Bandichhor, R.; Burgess, K. Spectral dispersion and water solubilization of Bodipy dyes via palladium catalyzed C-H functionalization. Org. Lett. 2007, 9, 2135−2138.

(42) Pallavicini, P.; Bernhard, C.; Dacarro, G.; Denat, F.; DiazFernandez, Y.; Goze, C.; Pasotti, L.; Taglietti, A. Optical method for predicting the composition of self-assembled monolayers of mixed thiols on surfaces coated with silver nanoparticles. Langmuir 2012, 28, 3558−3568.

(43) Kumar, D.; Meenan, J. B.; Dixon, D. Gluthathione-mediated release of Bodipy from PEG cofunctionalized gold nanoparticles. Int. J. Nanomed. 2012, 7, 4007−4022.

(44) Kumar, D.; Mutreja, I.; Meenan, J. B.; Dixon, D. Profile of polyload release from gold nanoparticles modified with Bodipy/PEG mixed monolayer. J. Nano Res. 2013, 25, 16−30.

(45) Peng, H.; Chen, W.; Cheng, Y.; Hakuna, L.; Strongin, R.; Wang, B. Thiol reactive probes and chemosensors. Sensors 2012, 12, 15907− 15946.

(46) Nagai, A.; Yoshii, R.; Otsuka, T.; Kokado, K.; Chujo, Y. Bodipybased chain transfer agent: reversibly thermoswitchable luminescent gold nanoparticles stabilized by Bodipy-terminated water-soluble polymer. Langmuir 2010, 26, 15644−15649.

(47) Theillet, F.-X.; Binolfi, A.; Fremdgen-Kesner, T.; Hingorani, K.; Sarkar, M.; Kyne, C.; Conggang, L.; Crowley, P. B.; Gierasch, L.; Pielak, G. J.; Elcock, A. H.; Gershenson, A.; Selenko, P. Physicochemical properties of cells and their effects on intrinsically disordered proteins (IDPs). Chem. Rev. 2014, 114, 6661−6714.

(48) Lee, E. S.; Gao, Z.; Bae, Y. H. Recent progress in tumor pH targeting nanotechnology. J. Controlled Release 2008, 132, 164−170.

(49) Chirico, G.; Beretta, S.; Baldini, G. Conformation of interacting lysozyme by polarized and depolarized light scattering. J. Chem. Phys. 1999, 110, 2297−2304.

(50) Tanaka, T. Experimental Methods in Polymer Science; Academic Press: London, 2000.

(51) Wang, Y.; Kuenzer, C. On gradient methods for maximum entropy regularizing retrieval of atmospheric aerosol particle distribution function. Proc. Appl. Math. Mech. 2007, 7, 1042103− 1042104.

(52) Levy, R.; Thanh, N. T. K.; Doty, R. C.; Hussain, I.; Nichols, R. J.; Schiffrin, D. J.; Brust, M.; Fernig, D. G. Rational and Combinatorial Design of Peptide Capping Ligands for Gold Nanoparticles. J. Am. Chem. Soc. 2004, 126, 10076−10084.

(53) Pallavicini, P.; Bernhard, C.; Chirico, G.; Dacarro, G.; Denat, F.; Dona, A.; Milanese, C.; Taglietti, A. Gold nanostars co-coated with thè Cu(II) complex of a tetraazamacrocyclic ligand. Dalton Trans. 2015, 44, 5652−5561.

(54) Montalti, M.; Prodi, L.; Zaccheroni, N.; Battistini, G. Modulation of the photophysical properties of gold nanoparticles by accurate control of the surface coverage. Langmuir 2004, 20, 7884− 7886.

(55) Bain, C. D.; Whitesides, G. M. Formation of two-component surfaces by the spontaneous assembly of monolayers on gold from solutions containing mixtures of organic thiols. J. Am. Chem. Soc. 1988, 110, 6560−6561.

(56) Bain, C. D.; Whitesides, G. M. Formation of monolayers by the coadsorption of thiols on gold: variation in the length of the alkyl chain. J. Am. Chem. Soc. 1989, 111, 7164−7175.

(57) Laibinis, P. E.; Fox, M. A.; Folkers, J. P.; Whitesides, G. M. Comparison of self-assembled monolayers on silver and gold − mixed monolayers derived from $HS(CH_2)_{21}X$ and $HS(CH_2)_{10}Y$ (X,Y= CH_3, CH_2OH) have similar properties. Langmuir 1991, 7, 3167−3173.

(58) Rumyantsev, E. V.; Alyoshin, S. N.; Martin, Y. S. Kinetic study of Bodipy resistance to acids and alkalis: Stability ranges in aqueous and non-aqueous solutions. Inorg. Chim. Acta 2013, 408, 181−185.

(59) Sironi, L.; Freddi, S.; Caccia, M.; Pozzi, P.; Rosetti, L.; Pallavicini, P.; Dona, A.; Cabrini, E.; Gualtieri, M.; Rivolta, I.; Panariti, A.; D′Alfonso, L.; Collini, M.; Chirico, G. Gold branched nanoparticles for cellular treatments. J. Phys. Chem. C 2012, 116, 18407−18418.

(60) Cavallaro, G.; Triolo, D.; Licciardi, M.; Giammona, G.; Chirico, G.; Sironi, L.; Dacarro, G.; Dona, A.; Milanese, C.; Pallavicini, P. Amphiphilic Copolymers Based on Poly[(hydroxyethyl)-D,L-aspartamide]: A Suitable Functional Coating for Biocompatible Gold Nanostars. Biomacromolecules 2013, 14, 4260−4270.